Hyperspectral anomaly detection: a comparative evaluation of methods

D. Borghys*[1], V. Achard[2], S.R. Rotman[3], N. Gorelik[3], C.Perneel[1], and E. Schweicher[4]

[1] Royal Military Academy, Signal And Image Centre, Brussels, Belgium

[2] French Aerospace Laboratory (ONERA), Toulouse, France

[3] Dept. of Elec. and Computer Eng. of the Ben-Gurion University of the Negev, Israel

[4] Royal Military Academy, Dept. CISS

E-mail: Dirk.Borghys@elec.rma.ac.be

Abstract

Anomaly detection in hyperspectral data has received a lot of attention for various applications. The aim of anomaly detection is to detect pixels in the hyperspectral datacube whose spectra differ significantly from the background spectra. In anomaly detection no prior knowledge about the target is assumed. Anomaly detection methods in general estimate the spectra of the background (locally or globally) and then detect anomalies as pixels with a large spectral distance w.r.t. the determined background spectra. Many types of anomaly detectors have been proposed in literature, each depending on several parameters. The aim of this paper is to compare the results of different types of anomaly detection when they are applied to scenes with different complexity: urban scenes with different complexity and rural scenes with sub-pixel anomalies. This paper only considers hyperspectral data in the VNIR and SWIR part of the EM spectrum ($\lambda = 0.4 - 2.5 \mu m$).

1 Introduction

Many types of anomaly detectors (ADs) have been proposed in literature [1]. The benchmark anomaly detector is the Reed-Xiaoli (RX) algorithm [2]. Different variations of this method have been proposed in literature [3, 4, 5, 6, 7]. This paper investigates the detection capabilities of two classes of anomaly detectors by comparing their results on a set of four datacubes of scenes with different complexities. The first class of examined detectors is the family of linear RX-based anomaly detectors. The second class consists of segmentation-based anomaly detection (SBAD) methods.

2 DataSet

The presented analysis was performed on a set of 4 hypercubes of scenes with varying complexity. Fig. 1 shows RGB composites of each of the datacubes used in this paper. Table 1 presents the main characteristics of the dataset. The first column is the name by which the scenes will be referred further in this paper. In the OBP and PAV scenes the anomalies are resp. aircraft and cars and the anomaly ground truth mask was determined by visual inspection. The two last datacubes are data from the Hymap sensor in which anomalies were inserted artificially. The two rightmost images in fig. 1 show these images with full-pixel anomalies. The results shown in this paper were obtained images with 10% mixing ratio sub-pixel anomalies.

Table 1: Overview of the dataset

Name	Site	Sensor name	Nr of bands	Waveband (μm)	Spatial resolution	Scene Description
OBP	Oberpfaffenhofen(Ge)	Hymap	126	0.44-2.45	4 m	Airfield with aerospace industry
PAV	Pavia (It)	Rosis	102	0.430-0.834	1.3 m	City
HAR	Hartheim (Ge)	Hymap	126	0.44-2.45	4 m	Agricutural area
CAM	Camargue (Fr)	Hymap	126	0.44-2.45	4 m	Agricutural area

978-1-4244-6051-9/11/$26.00

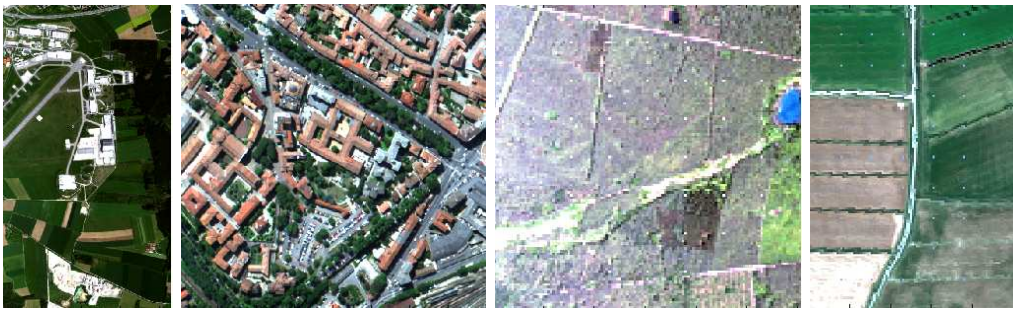

Figure 1: RGB composite of the original datacubes. From left to right: OBP, BJO, PAV, HAR and CAM

3 Anomaly detection methods

3.1 RX-based anomaly detectors

The RX detector [2] is a standard in anomaly detection. Basicly the RX detector calculates the Mahalanobis distance between the current pixel and the background:

$$D_{RX} = (r - \mu_B)^t C_B^{-1} (r - \mu_B) \tag{1}$$

C_B and μ_B are respectively the sample spectral covariance matrix and the spectral mean of the background pixels; r is the spectrum of the current pixel. Many different variations of the RX detector have been proposed in literature. They differ in the way the background covariance matrix and background mean is defined and estimated and also in the manner in which the inverse of the covariance matrix is implemented.

In **Global RX (GRX)** the spectral covariance matrix and spectral mean of the background is determined using the whole image and all spectral bands. In **Sub-space RX (SSRX)** the GRX is determined after PCA and the background statictics are determined on a limited number of PCA bands. Usually the first PCs are discarded in SSRX. In **OSPRX (RX after orthogonal subspace projection)** the background is defined by the first components of a singular Value Decomposition. These first components define the background subspace and the data are projected onto the orthogonal subspace before applying the RX detector [1]. In **Complementary Subspace Detector (CSD)** the highest variance PCs are used to define the background subspace and the others (the complementary subspace) as the taget subspace[4]. The PUT is then projected on the two subspaces and the anomaly detector is the difference of the projection onto the target subspace and the background subspace. Whitening is applied before applying the projection. The **Partialling Out RX detector (PORX)** partials out the effect of the clutter in a pixel component-wise by predicting each of its spectral components as a linear combination of its high-variance principal components. The detector applies then a Mahalanobis distance on the residual. These are all "global" methods: they use the whole scene for calculating the statistics. In **Local RX (LRX)** the covariance matrix and mean are determined locally in a window around the PUT. A double sliding window is used: a guard window and an outer window are defined and the background statistics are determined using the pixels between the two. **Quasi-local RX (QLRX)** offers an interesting compromise between the global and local RX approach. In QLRX the global covariance matrix is decomposed using eigenvector/eigenvalue decomposition[6]: $C = U\Lambda U^T$. The eigenvectors are kept in the RX, but the eigenvalues are replaced by the maximum of the local variance and the global eigenvalue. This means that the score of the detector will be lower at locations of the image with high variance (e.g. edges) than in more homogeneous areas. Spectral statistical standardisation is applied as pre-processing step. The local variance is determined in a double sliding window like in LRX.

3.2 Segmentation-based detectors

Because the scene is in most cases not described by a single Gaussian, neither locally and certainly not globally, anomaly detectors based on image segmentation have been proposed. Three global segmentation-based methods are used in this paper. In **Class-conditional RX (CCRX)** the image is first segmented, the global covariance matrix and mean within each class is determined before RX is applied. The Mahalanobis distance between the PUT and each of the class is determined. The final result is the minimum of these distances. In the current paper K-means clustering is used. In [8] a **self-organising map-based method (SOM)** is proposed: A trained SOM is considered as a representation of the background classes in the scene. Anomalies are determined by computing the spectral distances of the pixels from the SOM units. The SOM was applied on the first 3 PCA bands and run using a square map consisting of hexagonal cells. A **two-level end-member selection (TLES)** based method was also applied. The principle of this method [9] is the following: a small scanning window (typically 50×50 pixels) runs over the image and at each position of the window the principal background spectra are determined using a segmentation method based on end-member selection. Endmembers that correspond to a minimum percentage (MP) of the image tile are stored. At the end of the process an endmember selection is again applied on the stored endmembers and linear unmixing is applied on the image. Anomalies correspond to pixels with a large residue after unmixing.

4 Results and Discussions

The evaluation of the results is based on the receiver/operator curves (RoC curves). These are curves that plot the probability of detection (Pd) versus the probability of false targets (Pf). The evaluation measure is the area under the curve (AUC), i.e. the integral of the curve between Pf=0 and Pf=1. For all the algorithms, parameters were varied within a reasonable range and the shown results are the best results obtained for the algorithm. Table 2 shows the AUC results for all detectors for the four scenes. For GRX the values obtained without and with whitening are given. For the CSD whitening is always applied. For the other methods the results with or without whitening did not differ significantly; the values in the table are without whitening. In the datasets with a highly structured background, the best results are obtained by the SBAD methods. The best method is not always the same. In OBP the OSPRX also gives very good results. Note that for HAR and CAM the AUC gives the same results for several detectors. In order to distinguish them further, fig. 2 shows the RoC curves for these datasets. Pf is expressed in a logarithmic scale for highlighting better the difference at low values of Pf. In both HAR and CAM, LRX gives the best results. OSRRX and QLRX also give good results.

Site	RX-based AD							Segmentation-based AD		
	GRX	CSD	SSRX	OSPRX	PORX	LRX	QLRX	CCRX	SOM	TLES
OBP	0.866/0.827	0.962	0.975	**0.983**	0.933	0.518	0.956	0.902	0.862	**0981**
PAV	0.565/0.734	0.743	0.770	0.753	0.774	0.728	0.693	**0.832**	0.780	0.813
HAR	0.350/0.996	0.997	0.998	**0.999**	0.987	**0.999**	**0.999**	0.988	0.759	0.984
CAM	0.400/0.993	**0.999**	**0.999**	**0.999**	0.636	**0.999**	**0.999**	0.953	0.575	0.719

Table 2: Area under the RoC Curves for the different detectors

5 Conclusions

Results of various RX-based and segmentation-based anomaly detectors were compared in scenes with different compexity. Of the RX-based methods, OSPRX globally gives the best results. In highly structured scenes, SBAD methods give very good results, but the best SBAD method depends on the scene. For sub-pixel anomaly detection in a natural background, LRX, QLRX and OSPRX give the best results. All

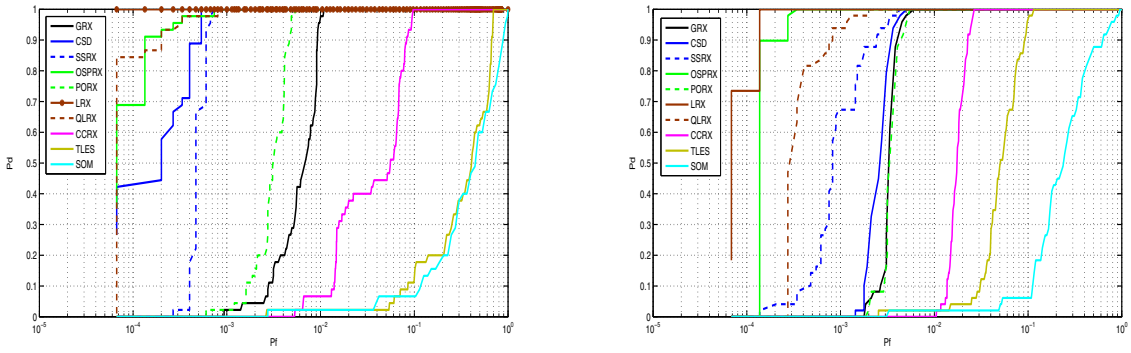

Figure 2: RoC curves for the different detectors for CAM10(left)and HAR10(right).

results are highly dependent on parameter settings and applied pre-processing method. These factors will be investigated in further work.

6 Acknowledgments

The OBP data acquisitions was sponsored by the Belgian Science Policy and flights were operated by the German Aerospace Agency DLR. PAV data were provided by Prof Gamba of Pavia Univ. The HAR scene is the courtesy of P. Wurteisen, European Space Agency, and the CAM image was provided by DLR.

References

[1] Matteoli, M. Diani, and G. Corsini, "A tutorial overview of anomaly detection in hyperspectral imagery," *IEEE A&S Systems Magazine, Part3: Tutorials*, vol. 21, no. 3, June 2010.

[2] I. Reed and X. Yu, "Adaptive multiband cfar detection of an optical pattern with unknown spectral distribution," *IEEE ASSP*, vol. 38, no. 10, pp. 1760–1770, Oct 1990.

[3] D. Stein, S. Beaven, L. Hoff, E. Winter, A. Schaum, and A. Stocker, "Anomaly detection from hyperspectral imagery," *IEEE Signal Proc. Mag.*, vol. 38, pp. 58–69, Jan 2002.

[4] A. Schaum, "Hyperspectral anomaly detection: Beyond rx," in *Proc. SPIE Algorithms and Technologies for Multispectral, Hyperspectral and Ultraspectral Imagery XII*, vol. 6565, 2007.

[5] E. Lo and A. Schaum, "A hyperspectral anomaly detector based on partialling out a clutter subspace," in *Proc. SPIE Algorithms and Technologies for Multispectral, Hyperspectral and Ultraspectral Imagery XV*, vol. 7334, 2009.

[6] C. Caefer, J. Silverman, O. Orthal, D. Antonelli, Y. Sharoni, and S. Rotman, "Improved covariance matrices for point target detection in hyperspectral data," *Optical Engineering*, vol. 47, no. 7, July 2008.

[7] H. Kwon and N. Nasrabadi, "Kernel rx-algorithm: A nonlinear anomaly detector for hyperspectral imagery," *IEEE-TGRS*, vol. 43, no. 2, pp. 388–397, Feb 2005.

[8] O. Duran and M. Petrou, "A time-efficient method for anomaly detection in hyperspectral images," *IEEE-TGRS*, vol. 45, no. 12, pp. 3894–3904, Dec 2007.

[9] D. Borghys, E. Truyen, M. Shimoni, and C. Perneel, "Anomaly detection in hyperspectral images of complex scenes." in *Proc. 29th Earsel Symposium*, Chania, June 2009.